

# Lawrence Berkeley National Laboratory

## Lawrence Berkeley National Laboratory

### **Title**

Design of a Nb<sub>3</sub>Sn Magnet for a 4th Generation ECR Ion Source

### **Permalink**

<https://escholarship.org/uc/item/40q0b1bg>

### **Author**

Prestemon, S,

### **Publication Date**

2008-08-17

Peer reviewed

# Design of a Nb<sub>3</sub>Sn Magnet for a 4th Generation ECR Ion Source

S. Prestemon, F. Trillaud, S. Caspi, P. Ferracin, G. L. Sabbi, C. M. Lyneis, D. Leitner, D. S. Todd, and R. Hafalia

**Abstract**—The next generation of Electron Cyclotron Resonant (ECR) ion sources are expected to operate at a heating radio frequency greater than 40 GHz. The existing 3rd generation systems, exemplified by the state of the art system VENUS, operate in the 10–28 GHz range, and use NbTi superconductors for the confinement coils. The magnetic field needed to confine the plasma scales with the rf frequency, resulting in peak fields on the magnets of the 4th generation system in excess of 10 T. High field superconductors such as Nb<sub>3</sub>Sn must therefore be considered. The magnetic design of a 4th. generation ECR ion source operating at an rf frequency of 56 GHz is considered. The analysis considers both internal and external sextupole configurations, assuming commercially available Nb<sub>3</sub>Sn material properties. Preliminary structural design issues are discussed based on the forces and margins associated with the coils in the different configurations, leading to quantitative data for the determination of a final magnet design.

**Index Terms**—ECR ion source, Nb<sub>3</sub>Sn superconducting magnets.

## I. INTRODUCTION

HIGH charge state ECR sources are essential components of future heavy-ion driver accelerators. Performance enhancements over existing technologies requires, among other technology developments, higher microwave frequencies and higher containment fields [1], [2]. The containment field is typically provided by a combination of sextupole fields, providing radial confinement, and solenoids, providing axial containment. The fields combine to form closed isosurfaces necessary for plasma confinement and RF power transfer. The requisite field strength is given by the resonance condition for an RF frequency  $f$  by

$$B_{\text{ECR}} = \frac{f}{28}, \quad (1)$$

with  $f$  in GHz and  $B_{\text{ECR}}$  in Teslas. Experience has shown that, whereas a closed surface of amplitude  $B_0 = B_{\text{ECR}}$  is necessary for electron resonance heating, an envelop of surfaces up to  $B_t \sim 2B_{\text{ECR}}$  is needed to contain the plasma for optimal performance. For 56 GHz operation this entails a closed surface field of  $B_t \sim 4$  T within the plasma chamber.

Manuscript received August 26, 2008. Current version published July 15, 2009. This work was supported by the Director, Office of Science, High Energy Physics, U.S. Department of Energy Contract DE-AC02-05CH11231.

The authors are with the Lawrence Berkeley National Laboratory, Berkeley, CA 94720 USA (e-mail: soprestemon@lbl.gov; ftrillaud@lbl.gov; s\_caspi@lbl.gov; pferracin@lbl.gov; GLSabbi@lbl.gov; cmlyneis@lbl.gov; DLeitner@lbl.gov; DSTodd@lbl.gov; RRHafalia@lbl.gov).

Color versions of one or more of the figures in this paper are available online at <http://ieeexplore.ieee.org>.

Digital Object Identifier 10.1109/TASC.2009.2017719

We begin with a simple review of ECR magnetic design, focusing on basic scalings that provide insight into the design process [3]. We then investigate two magnetic configurations based on the existing VENUS and SECAL [4] geometries, but leveraging the performance characteristics of recent Nb<sub>3</sub>Sn material developments. Advantages and disadvantages of each with respect to 56 GHz operation are presented. Finally, a modified VENUS geometry, designed to alleviate the limitations of the baseline case, is presented in terms of the magnetic performance.

A 2D structural model is then developed. High field magnets are typically limited as much by structural considerations as magnetic, and a mechanical design that provides sufficient control of prestress is critical to leverage high-performance superconductors. The structural model is analysed both for the baseline VENUS geometry and for the modified VENUS geometry, demonstrating improved behavior both in terms of magnetic margin and reduced peak stresses.

The first thing

## II. MAGNETIC DESIGN ISSUES

To provide some insight into the scaling of fields for an ECR source, it is useful to consider the case of idealized surface current distributions. The field amplitude generated by a pure order  $m$  multipole magnet (e.g. with line current density  $J'(\theta) = J'_0 \cos(m\theta)$  on a cylinder of radius  $R$ ) takes the general form (for  $r < R$ )

$$B_{\text{mod}}(r) = \frac{\mu_0 I_0}{R} \left( \frac{r}{R} \right)^{m-1}, \quad (2)$$

with total current per pole  $I_0 = J'_0 R/m$ .

For plasma containment magnetic pressure in the form of a field gradient  $\partial B/\partial r > 0$  is required, leading to the constraint  $m \geq 2$ . Note also that for a sextupole ( $m = 3$ ) the field increases with  $r^2$ , implying that space between the plasma chamber and the sextupole coil has a significant impact on the field seen by the superconducting magnet.

A well established magnetic design for an ECR source is to superimpose a sextupole field with a series of solenoids; the former provide radial confinement in the form of field isosurfaces on cylinders; the solenoids (*Injection* and *Extraction*, see Fig. 1) provide closure of the surfaces at the “ends”. To provide an isosurface of field amplitude  $B_{\text{ECR}}$  inside the  $B_t$  closed volume, the solenoid field must be sufficiently small (i.e. below  $B_{\text{ECR}}$ ) over an axial region. This is usually accomplished by having a third intermediate solenoid with opposite sign between the injection and extraction solenoids. An example of closed surfaces in an ECR source is provided in Fig. 2.

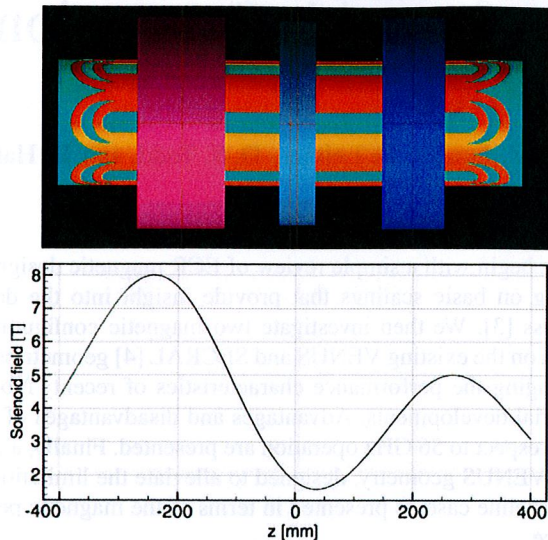


Fig. 1. Plot of the VENUS56 coil geometry (top) and corresponding solenoid field on-axis (bottom). The *Middle* solenoid serves to force the field amplitude down to provide a closed surface of  $B_{\text{mod}} = B_{\text{ECR}}$ . The *Injection* solenoid is on the left and the *Extraction* solenoid on the right.

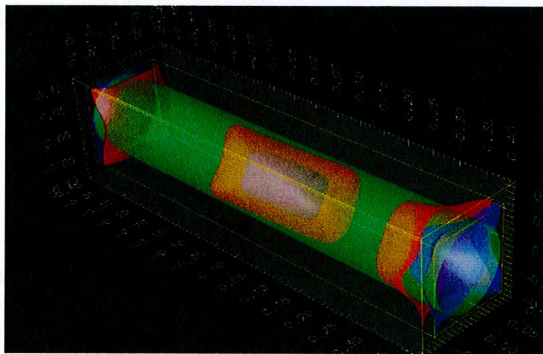


Fig. 2. Image of the closed surfaces  $\|B\| = \text{constant}$ . Green represents the  $r = 70$  mm plasma region; inside are two closed surfaces, the inner being defined by  $B_{\text{mod}} = B_{\text{ECR}}$ , and the outer by  $B_{\text{mod}} = 2.1B_{\text{ECR}}$ .

### A. Field Specifications

Two very distinct options can be pursued in terms of magnet design: sextupole-in-solenoid and solenoid-in-sextupole. The former is represented, for example, by the VENUS ECR at LBNL (see Fig. 1). The solenoid-in-sextupole configuration has also been used, an example being the SECRAL ECR. Since both the VENUS and the SECRAL magnet systems underwent some degree of design optimization, we analyse these two magnet geometries using  $\text{Nb}_3\text{Sn}$  material properties and assuming Rutherford cables to provide high superconductor fraction in the sextupole coils. The radial dimensions of the coils in the configurations considered here are provided in Table I. Note that in the SECRAL geometry the sextupole is placed directly on the solenoids so as to minimize the sextupole radius. The VENUS56w is a VENUS-style design modified to enhance load-line margin and reduce stresses. There are advantages to each design concept:

- The VENUS geometry leverages proximity of the sextupole to the closed surface location, minimizing peak

TABLE I  
RADIAL GEOMETRY OF THE SECRAL56, VENUS56, AND VENUS56W CONFIGURATIONS. ALL DIMENSIONS IN MILLIMETERS

	Sextupole		Injection		Middle		Extr.	
	r1	r2	r1	r2	r1	r2	r1	r2
SECRAL56	106	146	92	106	101	106	92	106
VENUS56	100	136	170	229	170	220	170	229
VENUS56W	100	160	194	253	194	244	194	253

TABLE II  
SYSTEM SPECIFICATIONS FOR COMPARISON ANALYSIS

Geometry		
	Inner diam. [mm]	Outer diam. [mm]
Plasma chamber	140	150
Warm bore	170	173.5
Innermost coil	204.5	
Magnetic field requirements		
Axial fields (solenoids) [T]		
Injection field	8	On axis
Minimum B field	1-2	On-axis
Extraction field	5	On-axis
Peak-to-Peak distance	50cm	
Radial field (sextupole) [T]		
Sextupole field	4.2	At $r = 70$ mm
Combined field [T]		
Last closed surface	> 4	At $r = 70$ mm

fields in that coil. However the sextupole magnet is subjected to radial fields from the solenoid ends, resulting in significant azimuthal forces with different symmetry than the sextupole field.

- The SECRAL geometry minimizes the influence of the solenoid on the sextupole field, at the expense of significantly higher field on the sextupole magnet surface due to the larger radius of the coils (see (2)). The sextupole field generates a large radial field on the solenoid that alternates sign azimuthally; the resulting Lorentz force distribution leads to sizable shear stresses within the solenoid.

For comparison purposes we impose specific field requirements at different spatial locations to satisfy ECR performance (see Table II). The current densities in all of the coils are therefore well defined, and the load-line fraction of critical current can be determined under assumptions of conductor performance and coil fabrication details.

The current densities and fields in each of the coils are provided in Table III. No iron is included in the model comparison. The solenoids in the SECRAL56 configuration are subjected to the large sextupole fields, resulting in high peak fields in all coils for that configuration. The high current densities in the SECRAL geometry solenoids stem from the drive to minimize the radius of the sextupole. In the VENUS geometry the solenoid field contributes predominantly a  $B_z$  field component on the sextupole. The field amplitude perpendicular to the current flow is provided for comparison. A modified VENUS56 geometry (VENUS56w) is also presented, designed to enhance magnetic margin and reduce stresses in the sextupole (see Section III).

### B. $\text{Nb}_3\text{Sn}$ and Cable Properties

There has been steady and significant improvement in  $\text{Nb}_3\text{Sn}$  properties over the last decade, based in large part on the DOE sponsored Conductor Development Program [5].

TABLE III  
56 GHz SYSTEM CHARACTERISTICS

Engineering current densities [ $A/mm^2$ ]				
	Sextupole	Injection	Middle	Extraction
SECRAL56	357.6	635	-75	547
VENUS56	455	256	166	208
VENUS56W	342	288	-250	238
Peak field [T]*				
SECRAL56	16.9	16.5	13.97	15.25
VENUS56	14.8 (13.0)	12.24	6.39	9.10
VENUS56W	15.34 (12.57)	13.35	8.57	10.31

\*Field amplitude orthogonal to current flow is provided in parenthesis

Rod-and-Restack Processed (RRP) wires developed by Oxford Science and Technology can now attain

$$J_c(12 \text{ T}, 4.2 \text{ K}) = 3000 \text{ A/mm}^2, \quad (3)$$

with filament sizes of  $D_{\text{eff}}$  below  $80 \mu\text{m}$ . To provide high engineering current densities the copper fraction of the  $\text{Nb}_3\text{Sn}$  wire is kept low, typically  $\text{Cu:NonCu} \sim 1$ , the value used in this study. Furthermore we assume that a Rutherford cable is used, resulting in an effective superconductor area fraction of 0.33 in the overall coilpack, as is typical of high-performance accelerator magnets. Scaling relations yielding  $J_c(H, T, \epsilon)$  for  $\text{Nb}_3\text{Sn}$  are fairly well established (see for example [6]).

Transport current in a type-II superconductor relies on flux pinning to contain the force acting on the vortices in the material. The vortices are subjected to an effective Lorentz force  $\vec{J} \times \vec{B}$ , so that field parallel to the current flow should not influence the pinning strength and hence transport current. Experiments measuring transport current under various applied field angle  $\theta$  describe a more complex scenario [7], with  $I_c(12 \text{ T}, 4.2 \text{ K})$  only doubling from  $\theta = \pi/2$  to  $\theta = 0$ .

### C. Load Line Analysis and Comparison

The field and current density data in Table III provide loadlines for the individual coils. An estimation of superconductor fraction in the coil cross-sections, together with superconductor  $J_c(H, T)$  scaling, allows determination of operating point feasibility. The SECRAL56 system requires current densities exceeding the capabilities of today's  $\text{Nb}_3\text{Sn}$  materials in both the sextupole and the injection solenoid. The VENUS56 geometry results in reasonable solenoid operating points, but little if any margin on the sextupole. The VENUS56w geometry enlarges the sextupole so as to "dilute" the current and recover some operating margin. The loadlines for the VENUS56w case are provided in Fig. 3. Despite the improved characteristics of the VENUS56w configuration, the system remains very challenging from a magnetic point of view.

## III. STRUCTURAL ANALYSIS

High field magnets are often limited by mechanical stresses due to the large integrated Lorentz forces. The combination of solenoid and sextupole fields in a 56 GHz ECR source results in a complex force distribution that must be understood and controlled. Based on the magnetic analysis of the VENUS and

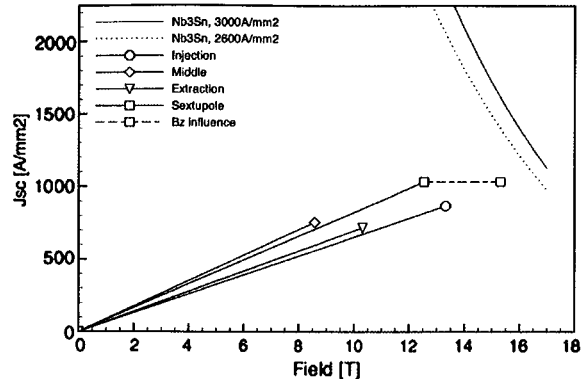


Fig. 3.  $J_c(B, 4.2\text{K})$  for RRP  $\text{Nb}_3\text{Sn}$ , and loadlines for the individual magnets in the VENUS56w case. Magnet engineering current densities are converted to superconductor current densities assuming  $A_{\text{sc}}/A_{\text{tot}} = 0.33$ . The dependence on applied field angle with respect to current flow direction suggests actual operating behavior lies in between the  $\|B_{\perp}\|$  and  $\|B\|$  values, illustrated by the  $B_z$ -influence line.

SECRAL configurations, we focus here on a 56 GHz modified VENUS geometry.

In the VENUS-type geometry the radial field from the solenoid ends adds significant azimuthal force to the sextupole coils, which must be accounted for in the structural design and analysis. Experience with high field accelerator magnets and solenoids indicates that the mechanical structure must provide sufficient prestress to minimize conductor motion and associated frictional heating during energization. The temperature differential from 300 K to 4.2 K can be leveraged to apply prestress by appropriate selection, sizing and placement of containment structures.

A shell-based structure using bladders and keys provides a mechanism for controlled room temperature prestress that is then amplified by thermal contraction during system cooldown. The use of bladders for prestress control was implemented in the VENUS magnet [8]. The method has been significantly developed for high-field accelerator magnets (see [9] for an example of a shell-based magnet system). The general assembly includes the following components (see Fig. 4):

- The sextupole coils are wound on titanium poles
- The coils are then surrounded by a titanium pad and key assembly that provides an interface to the solenoid system.
- A shared winding mandrel is used for the three solenoids. In the case of  $\text{Nb}_3\text{Sn}$  a reasonable choice of mandrel material is bronze, which is compatible with the wind-and-react process.
- The solenoid is surrounded by an iron pad and key assembly to provide an interface to the iron yoke.
- The iron yoke serves to a) return solenoid flux and reduce stray field and b) transmit force from the outer shell in towards the solenoid and sextupole coils
- The aluminum shell provides the majority of the prestress through differential contraction upon cooldown.

The assembly process requires a sequence of two bladder operations; first bladders between the sextupole and the solenoid are energized to install a key that provides force transmission from the solenoid to the sextupole. A second bladder operation is performed to install keys between the solenoid and the shell

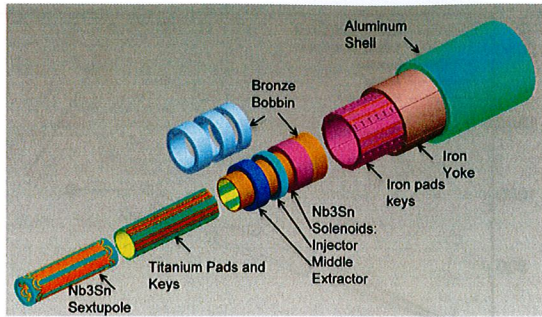


Fig. 4. Assembly layout for a 56 GHz  $\text{Nb}_3\text{Sn}$  ECR source.

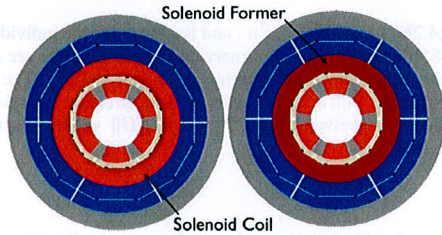


Fig. 5. Mechanical model of a "center" (left) and "end" (right) cross-section.

TABLE IV  
VENUS56W MECHANICAL ANALYSIS. AZIMUTHAL STRESSES IN THE SEXTUPOLE DURING ASSEMBLY PHASES, COOLDOWN, AND ENERGIZATION. "AVERAGE" IS DEFINED AS THE VALUE AT MID-RADIUS ON THE POLE

Load step	Sextupole center		Sextupole end	
	Average	Maximum	Average	Maximum
<b>Assembly (<math>\sigma_\theta</math>, [MPa])</b>				
Step I	-30 (-45)	-52 (-92)	-44 (-55)	-77 (-111)
Step II	-71 (-90)	-100 (-135)	-61 (-77)	-85 (-114)
<b>Cooldown and Energization (<math>\sigma_\theta</math>, [MPa])*</b>				
Cooldown	-118 (-146)	-159 (-177)	-101 (-121)	-138 (-149)
Energization	0	-86 (-118)	0	-175 (-212)

Values in parenthesis refer to VENUS56 geometry.

structure, resulting in an integrated system transmitting force from the shell to the sextupole, via the solenoid.

The essential mechanical behavior of the system can be analysed using two 2D cross sections that characterize two critical regions of the system (see Fig. 5):

- At the axial "center" of a solenoid the solenoid field is parallel to the sextupole current. At this location the solenoid is subjected to a large radial Lorentz force, resulting in a reduction of applied compressive force transmitted to the sextupole.
- At the solenoid "end" the radial solenoid field superimposed on the sextupole coil introduces a significant additional azimuthal force on the sextupole coil.

In both cases significant additional prestress is required, beyond that needed by the sextupole coil alone. A structural analysis, consisting of sequential analysis of assembly, cooldown, and energization states in the "center" and "end" regions, has been performed. Optimized key interference to eliminate coil separation results in high, but marginally acceptable, peak stresses in the sextupole coils (see Table IV). As an example, the final stress state in the sextupole under full system energization is shown in Fig. 6.

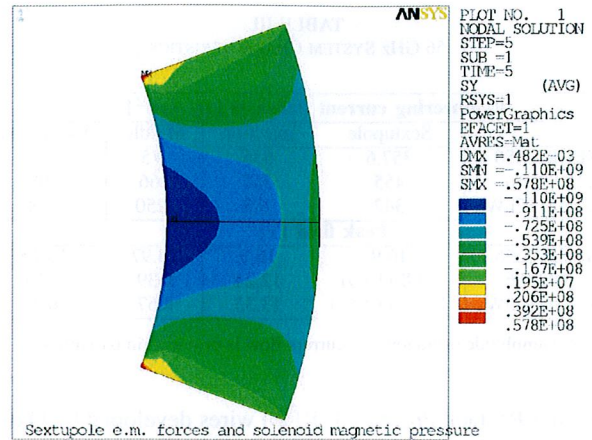


Fig. 6. Azimuthal stress distribution in the sextupole in the "center" cross-section under full-current excitation.

#### IV. CONCLUSION

The magnetic and structural investigation of a magnet system for a 56 GHz ECR ion source has been undertaken. Preliminary results suggest that the fields can be generated using the latest high-field  $\text{Nb}_3\text{Sn}$  conductors and magnet structural support and fabrication processes. The system is challenged both magnetically, in terms of current margin, and structurally, requiring large prestress and operating stress. The design is only realistic with the use of the latest  $\text{Nb}_3\text{Sn}$  conductor developments; the proposed design could not have been pursued a few years ago. The structural design leverages concepts and components developed by the LBNL Superconducting Magnet Program, in particular the shell and bladder structure that has been developed for high-field accelerator magnets and successfully demonstrated on record-breaking prototype magnets. The combination of nested coils requires transmission of prestress through the solenoid to the sextupole. The proposed assembly provides a prestress mechanism through a 2-step bladder-and-key approach that appears feasible, but has yet to be applied to a real magnet system. Although very aggressive, preliminary analysis suggests the fabrication of a 56 GHz ECR source is feasible using available superconductors.

#### REFERENCES

- [1] D. Leitner *et al.*, "Progress and perspective for high frequency, high performance superconducting ecr ion sources," in *Proceedings, 18th Int. Conf. Cyclotron and Their Applications, Giardini Naxos, 2007*, p. 265.
- [2] S. Gammino, *High Energy Phys. Nucl. Phys.* vol. 31, p. 137, 2007.
- [3] C. M. Lyneis *et al.*, "Fourth generation electron cyclotron resonance ion sources (invited)," *Rev. Sci. Instrum.*, vol. 79, no. 2, p. 02A321, Jan. 2008.
- [4] H. W. Zhao *et al.*, *Chinese Physical Society* vol. 31, pp. 8–12, 2006.
- [5] D. R. Dietderich and A. Godeke, "Nb<sub>3</sub>Sn research and development in the USA—wires and cables," *Cryogenics*, vol. 48, p. 331, 2008.
- [6] A. Godeke, B. ten Haken, H. H. J. ten Kate, and D. C. Larbalestier, "A general scaling relation for the critical current density in Nb<sub>3</sub>Sn wires," *Supercond. Sci. and Techn.*, vol. 19, p. R100, 2006.
- [7] A. Godeke *et al.*, in *Inst. Phys. Conf.*, 1997, no. 158.
- [8] C. E. Taylor *et al.*, *IEEE Trans. Appl. Supercond.*, vol. 10, no. 1, p. 224, 2000.
- [9] P. Ferracin *et al.*, *IEEE Trans. Appl. Supercond.*, vol. 17, no. 2, 2007.